Gene Expression Profiling of MCF10A Breast Epithelial Cells Exposed to IOERT

LUIGI MINAFRA[1*], VALENTINA BRAVATÀ[1*], GIORGIO RUSSO[1], GIUSI IRMA FORTE[1],
FRANCESCO PAOLO CAMMARATA[1], MARILENA RIPAMONTI[1],
GIULIANA CANDIANO[1], MELCHIORRE CERVELLO[2], AGATA GIALLONGO[2],
GIOVANNI PERCONTI[2], CRISTINA MESSA[1,4,5] and MARIA CARLA GILARDI[1,3,5]

[1]Institute of Bioimaging and Molecular Physiology,
National Research Council (IBFM-CNR) -LATO, Cefalù, Italy;
[2]Institute of Biomedicine and Molecular Immunology "Alberto Monroy" -
National Research Council (IBIM-CNR), Palermo, Italy;
[3]Nuclear Medicine, San Raffaele Scientific Institute, Milan, Italy;
[4]Nuclear Medicine Center, San Gerardo Hospital, Monza, Italy;
[5]Department of Health Sciences, Tecnomed Foundation, University of Milano-Bicocca, Milan, Italy

Abstract. *Background/Aim: Intraoperative electron radiation therapy (IOERT) is a therapeutic approach that delivers a single high dose of ionizing radiation (IR) directly to the tumor bed during cancer surgery. The main goal of IOERT is to counteract tumor growth by acting on residual cancer cells as well as to preserve healthy surrounding tissue from the side-effects of radiation therapy. The radiobiology of the healthy tissue response to IR is a topic of interest which may contribute to avoiding impairment of normal tissue and organ function and to reducing the risks of secondary cancer. The purpose of the study was to highlight cell and gene expression responses following IOERT treatment in the human non-tumorigenic MCF10A cell line in order to find new potential biomarkers of radiosensitivity/radioresistance.*
Material and Methods: Gene-expression profiling of MCF10A cells treated with 9 and 23 Gy doses (IOERT boost and exclusive treatment, respectively), was performed by whole-genome cDNA microarrays. Real-time quantitative reverse transcription (qRT-PCR), immunofluorescence and immunoblot experiments were carried out to validate candidate IOERT biomarkers. Clonogenic tests and morphological evaluations to examine cellular effects induced by radiation were also conducted. Results: The study revealed a dose-dependent gene-expression profile and specific key genes that may be proposed as novel markers of radiosensitivity. Our results show consistent differences in non-tumorigenic cell tolerance and in the molecular response of MCF10A cells to different IOERTs. In particular, after 9 Gy of exposure, the selection of a radioresistant cell fraction was observed. Conclusion: The possibility of clarifying the molecular strategies adopted by cells in choosing between death or survival after IR-induced damage opens-up new avenues for the selection of a proper personalized therapy schedule.

This article is freely accessible online.

*These Authors contributed equally to this study.

Correspondence to: Valentina Bravatà and Luigi Minafra, Institute of Bioimaging and Molecular Physiology, National Research Council (IBFM-CNR) -LATO, Cefalù (PA), Italy. E-mail: valentina.bravata@ibfm.cnr.it and luigi.minafra@ibfm.cnr.it.

Intraoperative electron radiation therapy (IOERT) differs from conventional radiotherapy (RT), since a large dose of ionizing radiation (IR) is employed in a single fraction directly to the tumor bed during cancer surgery, either as an exclusive treatment of 21-23 Gy or as an advanced boost of 9-12 Gy. The use of IOERT for breast cancer (BC) treatment has increased due to the development of the partial breast irradiation (PBI) strategy with the intent of avoiding tumor recurrence. This segmental RT replaces whole-breast irradiation and is based on the discovery that approximately 85% of local relapses are localized to the same breast quadrant from which the primary tumor was removed (1-6). Preliminary results of PBI with IOERT, both as a boost and as an exclusive treatment, seem to be promising in terms of local disease control, however few data have been collected on long-term toxicity, as well as molecular stress mechanisms specifically induced by high-

dose treatments (7-9). IR, both as X-rays, mainly used in conventional external-beam RT, and high-energy electrons generated by linear accelerators in IOERT, cause cell injury to both tumor and normal cells, producing a disequilibrium in the survival/cell death decision (9-11). Increasing evidence suggests that different factors, including the type of radiation and dose, are primarily important in radiation response, related also to the cell type. However, factors establishing the specific cellular fate after IR exposure have not been clearly defined. In addition, it has been shown that cell death induction is a very complex mechanism accounting for the different effects of IR, and cell death modality is not unique in response to radiation in cancer and normal cells (11-13). Several IR-induced genes trigger complex intracellular signaling pathways controlling many processes, such as cell-cycle progression, survival and cell death, DNA repair and inflammation (13-15). Nevertheless, the contribution of these genes and regulatory networks involved in the cellular response to high radiation doses is not completely understood. Despite the great interest of the scientific community on the clinical application of IOERT in BC, very few studies describe the effects of IOERT and particularly the molecular mechanisms of radiation toxicity in normal breast tissue. The gene-expression profiles of non-tumorigenic breast cells treated with high IR doses, such as those used during IOERT need to be further evaluated (16-17). It should also be taken into account that BC is a heterogeneous and complex disease at both molecular and clinical levels. Thus, on the one hand, the failure of radiation treatments associated with cell radioresistance may occur and on the other, effects due to radiosensitivity of the normal tissue surrounding the tumor may be present (18-21).

Recently, we investigated cell response and gene-expression profiles activated by IOERT treatments in the human MCF7 BC cell line and designed two network models induced by 9 and 23 Gy doses using the selected and validated genes. We reported a dose-dependent transcriptome change that regulates cell-fate decisions in two different ways, according to the doses used. IOERT treatments inhibited the growth and proliferation of MCF7 cells, and the post-irradiation cell traits reflected a typical senescent phenotype (22).

In order to assess the toxic effects of IOERT treatment and to select for potential new biomarkers of radiosensitivity/radioresistance, we describe cell and gene-expression responses of the non-tumorigenic mammary MCF10A cell line, used as a model of normal breast epithelial cells, following exposure to 9 and 23 Gy doses.

Understanding the molecular mechanisms of radiation toxicity is critical for the development of counter-measures for radiation exposure, as well as for improvement of clinical radiation effects in cancer treatment.

Materials and Methods

IOERT treatment. The NOVAC7 (Sortina Iort Technologies, Vicenza, Italy) IOERT system was used to perform treatments at different tissue depths. The beam collimation was performed through a set of polymethylmethacrylate applicators: cylindrical tubes with a diameter ranging from 3 to 10 cm and face angle of 0°-45°. The electron accelerator system was calibrated under reference conditions, cell-irradiation setup and the dose distribution were conducted as previously reported (22). IOERT cell treatments were carried out at two dose values, 9 Gy (in boost scheme) and 23 Gy (according to the exclusive modality) to the 100% isodose at a dose rate of 3.2 cGy/pulse.

Cell culture and clonogenic survival assay. The human non-tumorigenic breast epithelial MCF10A cell line was purchased from the American Type Culture Collection (Manassas, VA, USA) and cultured at 37°C in an incubator with 5% CO_2 according to the supplier's instructions. All cell culture media and supplements were obtained from Invitrogen (Carlsbad, CA, USA). Cells were seeded in 100-mm Petri dishes or in 24-well plates 48 h before treatments and at sub-confluence were irradiated. Twenty-four hours after irradiation, clonogenic survival assay was performed according to the protocol of Franken *et al*. (23), as previously described (22). The surviving fraction (SF) of irradiated cells was normalized to the plating efficiency (PE) of untreated control cells (basal). Data represent the average SF±standard deviation (SD) of three biologically independent experiments. Moreover, in order to evaluate cell radiation effects, cells throughout the course of the assays were monitored for cell morphology and growth pattern by photographing five random fields for each treatment under a Zeiss Axiovert phase-contrast microscope (Carl Zeiss, Göttingen, Germany).

Gamma-H2AX immunofluorescence analysis. Cells were grown on glass coverslips to reach 70% confluency before treatment and control cells (basal, *i.e.* untreated) were grown in parallel. After defined times, cells were processed for immunofluorescence, as previously described (22). The images were acquired by a Nikon Eclipse 80i (Chiyoda, Tokyo, Japan). γH2AX quantification was performed by ImageJ analysis software (http://rsb.info.nih.gov/ij/).

Whole-genome cDNA microarray expression analysis. Gene expression profiling of MCF10A cells treated with 9 and 23 Gy IR doses were performed. Twenty-four hours after each treatment, MCF10A cells were harvested, counted and the pellet stored immediately at −80°C. RNA extraction, quantification and purity evaluation were performed as previously described (22). Gene-expression profiles of MCF10A cells treated with 9 Gy and 23 Gy were carried-out according to Agilent Two-Color Microarray-Based Gene Expression Analysis protocol as described recently by our group (22). Seven replicates were performed. Statistical data analysis, background correction, normalization and summary of expression measure were conducted with GeneSpring GX 10.0.2 software (Agilent Technologies) as previously reported (22). Genes were identified as being differentially expressed if they showed a fold-change (FC) of at least 1.5 and a *p*-value for the difference of less than 0.05 compared to untreated MCF10A cells used as reference sample. The data discussed here have been deposited in Gene Expression Omnibus of National Center for Biotechnology Information (NCBI) link (24) and are accessible through GEO Series accession number (http://www.ncbi.nlm.nih.gov/

Table I. *Primer sequences used for Real-Time Quantitative Reverse Transcription PCR analyses.*

Gene symbol	Gene name	Forward primer 5'>3'	Reverse primer 5'>3'	Template size (base pairs)
AURKA	Aurora kinase A, transcript variant 1	cccaccttcggcatcctaata	tgactgaccacccaaaatctgc	279
CASP8	Caspase 8, apoptosis-related cysteine peptidase	ggctttgaccacgacctttg	tatcccctgacaagcctga	287
CCNB1	Cyclin B1 (CCNB1), mRNA [NM_031966]	caactgcaggccaaaatgcct	cttcttctgcagggcacat	259
CDC20	Cell division cycle 20	ctgtctgagtgccgtggat	cgcagggtccaactcaaaac	262
CDC25C	Cell division cycle 25 C	tctggccaaggaaagctcag	cgacagtaaggcagccact	207
CDKN1A/p21	Cyclin-dependent kinase inhibitor 1A (p21, CIP1)	cggcttcatgccagctactt	tcaccctgcccaaccttaga	245
CDKN3	Cyclin-dependent kinase inhibitor 3	ttctgcaccagaggggaact	caggctgtctatggcttgct	282
CENPF	Centromere protein F, 350/400kDa (mitosin)	cgcattgaggccgatgaaaag	ttcaggcttctggccatctc	218
CXCR3	Chemokine (C-X-C motif) receptor 3	gcatcagctttgaccgctac	ggcatagcagtaggccatga	278
GADD45B	Growth arrest and DNA-damage-inducible, beta	ggctctctggctcggatttt	acgctgtctgggtccacatt	239
GTSE1	G-2 and S-phase expressed 1	acagattccaggctggtgga	gcttgcagcatctggagtga	228
HIST1H4B	Histone cluster 1, H4b	gataacatccaaggcatcacca	ctgagaagggcctttgagga	266
HIST1H4C	Histone cluster 1, H4c	gtgctaagcgccatcgtaag	ctgtgacagttttgcgcttgg	207
HIST1H4D	Histone cluster 1, H4d	gtcaagcgtatttctggcctc	ccgttggttttgcggtagtgt	219
KIF2C	Kinesin family member 2C	acggagatccgtcaactcca	tctcctcgctgaccatcct	230
KRT1	Keratin 1	cgacctggacagcatcattg	catccttgagggcattctcg	284
KRT16	Keratin 16	tccagggactgattggcagt	gaagacctcgcgggaagaat	209
LMNB1	Lamin B1	ccttcttcccgtgtgacagt	cctcccattggttgatcctg	224
MLL	Lysine (K)-specific methyltransferase 2A	actccccttccttcacct	atccaccttgggtcccctta	299
NDC80	NDC80 kinetochore complex component	ggtcgtgtcaggaaactgga	aagtggtctcgggtcctga	293
NEK2	NIMA-related kinase 2	ccattggcacaggctccta	agccagatcccctcctcca	248
NOTCH1	Notch 1	agctgcatccagaggcaaac	tggttctggagggaccaaga	268
PLK1	Polo-like kinase 1	tgccacctccagtgacatgct	cagtgccgtcacgctctat	265
PYGO	Pygopus family PHD finger 1	atttgaagccttgcagcagactt	ggagctttaccagcctccaat	246
TP53INP	Tumor protein p53 inducible nuclear protein 1	tgctgagccatccactctga	tccctgcatcaagccactac	232
ZDHHC15	Zinc finger, -type containing 15	tgcagggctcacagttacca	ggtgccacaggaggtaatg	282

geo/query/ acc.cgi?acc=GSE65954). Microarray data are available in compliance with Minimum Information About a Microarray Experiment standards.

MetaCore network analyses. Gene expression profiles of IOERT-treated MCF10A cells were also analyzed by pathway analysis using the network building tool MetaCore (Thomson Reuters, Philadelphia, PA, USA) consisting of millions of relationships between proteins derived from publications about proteins and small molecules (including direct protein interaction, transcriptional regulation, binding, enzyme-substrate, and other structural or functional relationships). Results, *i.e.* maps of protein lists from the uploaded dataset, were then compared with all the possible pathway maps for all the proteins in the database, and the *p*-value was calculated based on the hypergeometric distribution probability test. The most representative networks that were significantly changed were selected and analyzed.

Real-Time Quantitative Reverse Transcription PCR. Candidate genes for qRT-PCR analysis were chosen based on the microarray results. One microgram of total RNA was reverse-transcribed into cDNA and analyzed by real-time PCR as previously described (22). The oligonucleotide primers were selected with Primer3 software (25-26) and tested for their human specificity using the NCBI database. Primer sequences (forward and reverse) used are listed in Table I. Quantitative data, normalized *versus* 18S rRNA gene, were analyzed by the average of triplicate cycle thresholds (Ct) according to the $2^{-\Delta\Delta ct}$ method using SDS software (Applied Biosystems, Carlsbad,

CA). The data shown were generated from three independent experiments and the values are expressed relative to mRNA levels in the untreated MCF10A cells used as control sample as the mean±SD.

Western blot analysis. Whole-cell lysates from 4 to 6×10^6 treated and untreated cells were collected as recently described (22). Western blots experiments were performed as previously reported (22). The following primary antibodies were used: β-actin (Sigma, St. Louis, MO, USA); poly (ADP-ribose) polymerase 1 (PARP), Polo-like kinase 1 (PLK1), phospho-epidermal growth factor receptor (Cell Signaling Technologies, Danvers, MA, USA); and pro-caspase-8, EGFR, p53, c-MYC, (Santa Cruz, Biotechnology Inc, Heidelberg, Germany).

Results

Clonogenic assay and morphological analysis. In order to assess MCF10A cell viability in terms of reproductive capacity after IOERT, clonogenic survival assays were performed. Twenty-four hours post-irradiation with 9 and 23 Gy doses, cells were seeded appropriately, maintained under normal culture conditions and analyzed at two to three weeks later for the formation of colonies. The results showed that 23 Gy exposure inhibited the growth and proliferation of MCF10A cells, as colony-forming ability was markedly impaired by irradiation and no colonies were observed. On the contrary,
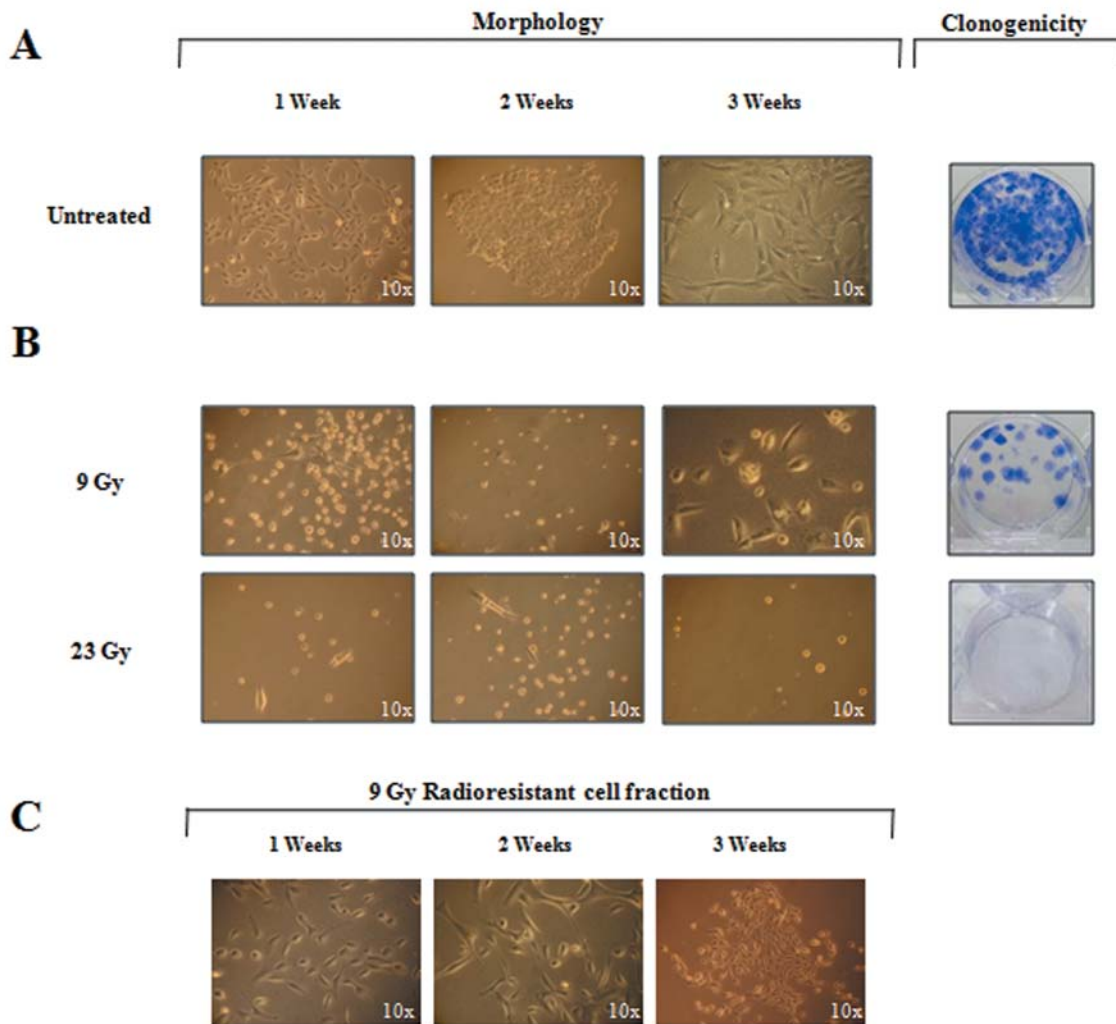
Figure 1. *Micrographs (×10) of MCF10A cells in culture after 1, 2, and 3 weeks post-Intraoperative electron radiation therapy (IOERT) for morphological evaluation and clonogenic survival assay: A: Untreated cells; B: MCF10A cells treated with 9 Gy and 23 Gy; C: radioresistant surviving fraction of MCF10A cells treated with 9 Gy.*

following the 9-Gy boost treatment, an SF of 9.6% was found, indicating the selection of a surviving radioresistant cell fraction with reproductive capacity (Figure 1A and 1B).

In order to evaluate the effects of IOERT on cell morphology, throughout the course of the clonogenic assays, cells were observed under phase-contrast microscopy and random fields for each treatment were photographed. After irradiation with 9 Gy and 23 Gy doses, the response of MCF10A cells in terms of morphology was similar. Cell damage at both the membranous and cytoplasmic levels was observed, starting 72 h post-treatment and increasing within one week. The total detachment of MCF10A cells treated with 23 Gy from the culture substrate occurred progressively from two to three weeks. In the case of MCF10A cells treated with 9 Gy, a radioresistant growing cell fraction, which we

maintained in culture up to three weeks post-treatment, was also observed (Figure 1C). Moreover, unlike IOERT-treated MCF7 cells (22), MCF10A cells did not exhibit morphology of a radiation-induced senescent phenotype. Indeed, biochemical tests for senescence-associated β-galactosidase activity did not reveal any cellular senescence activation in response to IOERT (data not shown).

γ-H2AX immunofluorescence analysis. Following exposure to IR, histone H2AX is immediately phosphorylated at serine 139 (γ-H2AX) with consequent foci formation as a sensitive early cell response to the presence of DNA double-strand breaks. To evaluate the time course of the appearance of γ-H2AX foci in MCF10A cells upon IOERT, we performed direct immunofluorescence analyses after 0.5, 1, 3, 6 and 24 h

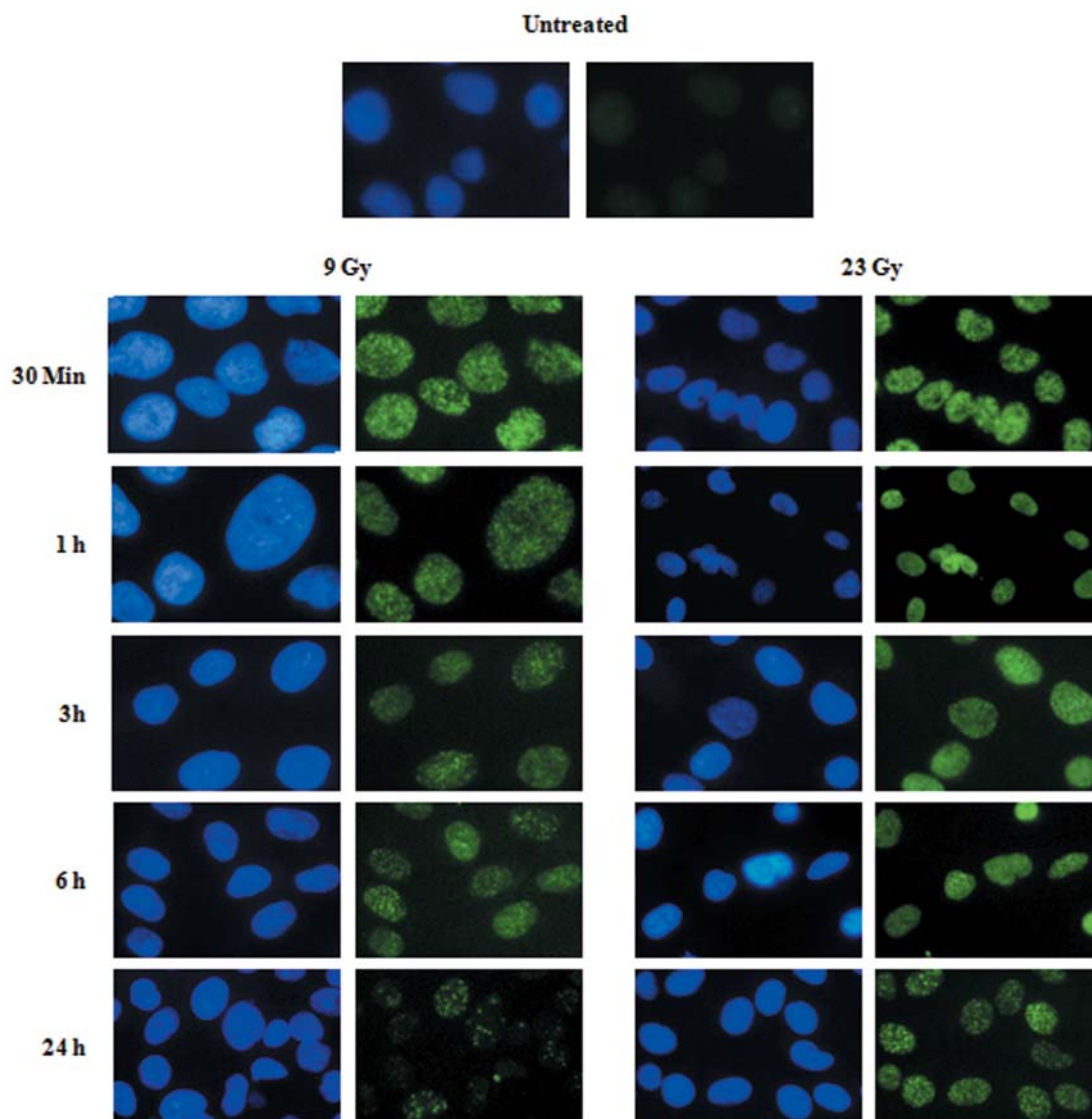Figure 2. *Micrographs (×20) of gamma-H2AX immunofluorescence (γH2AX) analysis in MCF10A cells after 30 minutes, and 1, 3, 6, and 24 h exposure to 9 and 23 Gy doses.*

of exposure to 9 and 23 Gy IR doses. γ-H2AX foci formation occurred within 30 min of irradiation at 9 and 23 Gy doses. In particular, in MCF10A cells treated 9 Gy, the number of foci gradually decreased at 6 and 24 h post-treatment, whereas in MCF10A cells treated with 23 Gy, it remained high with respect to untreated cells at 24 h after irradiation (Figures 2 and 3). These results suggest that foci formation in MCF10A cells was rapid, with a dose-dependent increase following exposure to IOERT.

Overview of cDNA microarray gene expression. In this study, a Two-Color Microarray-Based Gene Expression Analysis (Agilent Technologies) was conducted on 9 Gy- and 23 Gy-treated MCF10A cells using untreated MCF10A cells as a reference sample. Comparative differential gene-expression analysis revealed that in MCF10A cells treated with 9 Gy, expression levels of 72 genes were significantly altered, by 1.5-fold or greater, compared to the untreated MCF10A cell reference group: 18 genes were down-regulated and 54 were up-regulated. Moreover, comparative differential gene-expression analysis revealed that 451 genes in MCF10A cells treated with 23 Gy had significantly altered expression levels compared to the untreated MCF10A reference group: 226 genes were down-regulated and 225 were up-regulated (GSE65954). Up- and down-regulated transcripts were selected and grouped according to their involvement in

Table II. *Up- and down-regulated genes in MCF10A cells treated with 9 Gy.*

MCF10A cells treated with 9 Gy

Gene symbol	Gene ID	Description	Fold change by microarray	Fold change by qRT-PCR
AURKA	6790	Aurora kinase A, transcript variant 1	1.66	1.4
CDC20	991	Cell division cycle 20	1.95	2.5
CDC25C	995	Cell division cycle 25 C	1.62	1.7
CENPF	1063	Centromere protein F, 350/400kDa (mitosin)	1.68	4.8
CXCR3	2833	Chemokine (C-X-C motif) receptor 3	−5.02	0.62
GTSE1	51512	G-2 and S-phase expressed 1	2.00	1.3
KIF2C	11004	Kinesin family member 2C	1.69	1.7
KRT1	3848	Keratin 1	1.70	2.6
KRT16	3868	Keratin 16	1.54	1.3
MLL	4297	Lysine (K)-specific methyltransferase 2A	−1.62	0.31
PLK1	5347	Polo-like kinase 1	1.92	9.9
PYGO	26108	Pygopus family finger 1	6.03	1.3
ZDHHC15	158866	Zinc finger, -type containing 15	-3.32	0.16

Table III. *Up- and down-regulated genes in MCF10A cells treated with 23 Gy.*

MCF10A cells treated with 23 Gy

Gene symbol	Gene ID	Description	Fold change by microarray	Fold change by qRT-PCR
CASP8	841	Caspase 8, apoptosis-related cysteine peptidase	1.93	3.5
CCNB1	891	Cyclin B1 (CCNB1), mRNA [NM_031966]	−1.96	0.59
CDKN1A/p21	1026	Cyclin-dependent kinase inhibitor 1A (p21, CIP1)	1.58	5.9
CDKN3	1033	Cyclin-dependent kinase inhibitor 3	−2.18	0.81
GADD45B	4616	Growth arrest and DNA-damage-inducible, beta	1.58	1.6
HIST1H4B	8366	Histone cluster 1, H4b	−1.67	0.57
HIST1H4C	8364	Histone cluster 1, H4c	−1.58	0.28
HIST1H4D	8360	Histone cluster 1, H4d	−1.63	0.33
LMNB1	4001	Lamin B1	−1.70	0.7
NDC80	10403	NDC80 kinetochore complex component	−1.98	0.43
NEK2	4751	NIMA-related kinase 2	−2.79	0.86
NOTCH1	4851	Notch 1	1.72	4.7
PLK1	5347	Polo-like kinase 1	−2.38	0.8
TP53INP	94241	Tumor protein p53 inducible nuclear protein 1	1.60	8.2

specific biological pathways using integrated pathway enrichment analysis with GeneGo MetaCore. Data sets were loaded into Metacore software and the top enriched canonical metabolic pathways were analyzed. The result of this mapping revealed involvement of a set of factors controlling specific networks such as regulation of cellular process, inflammation, tissue degradation, cell-cycle modulation, and chromatin modification in comparison to the reference sample. Candidate genes were selected, validated and analyzed using the PubMatrix tool, as previously described (22, 27).

Microarray validation experiments. Genes for microarray validation experiments were chosen based on two considerations: i) factors known to be modulated by IR; and ii)

less-known genes involved in cell response to high radiation doses for proposal as new molecular markers. In order to identify possible documented relationships between microarray gene-expression lists and processes known to be involved in cell response to IR treatment, we used the PubMatrix V2.1 tool. In this way, bibliographic relationships between differentially expressed genes and some selected queries such as IR, radiation, cancer, BC, apoptosis, inflammation, DNA damage and DNA repair were analyzed. Moreover, based on the microarray data set, the PubMatrix results and MetaCore analyses, we chose 27 candidate genes and performed qRT-PCR validation experiments (Tables II and III). In MCF10A cells treated with 9 Gy, 13 selected genes were validated: 10 genes were up-regulated and among these, the following seven genes were

described as being involved in the positive regulation of the cell cycle and nuclear division: *G₂ and S-phase expressed 1* (*GTSE1*), *Aurora kinase A, transcript variant 1* (*AURKA*), *Cell division cycle 20* (*CDC20*), *CDC25C, PLK1, Centromere protein F, 350/400kDa (mitosin)* (*CENPF*) and *Kinesin family member 2C* (*KIF2C*) (Table II). As also shown in Table II, the following three genes were down-regulated: Lysine (K)-specific methyltransferase 2A (*MLL*), Chemokine (C-X-C motif) receptor 3 (*CXCR3*) and Zinc finger, -type containing 15 (ZDHHC15). On the other hand, in MCF10A cells treated with 23 Gy, 14 selected genes were validated. As shown in Table III, five genes were up-regulated: Caspase 8, apoptosis-related cysteine peptidase (*CASP8*), Cyclin-dependent kinase inhibitor 1A (p21, CIP1) (*CDKN1A/p21*), Growth arrest and DNA-damage-inducible, beta (*GADD45B*), Notch 1 (*NOTCH1*) and tumor protein p53 inducible nuclear protein 1 (*TP53INP*); while nine genes of the histone cluster and involved in cell-cycle modulation, such as CCNB1, CDKN3, Histone cluster 1, H4b (*HIST1H4B*), HIST1H4C, HIST1H4D, Lamin B1 (*LMNB1*), NDC80 kinetochore complex component (*NDC80*), NIMA-related kinase 2 (*NEK2*) and PLK1, were down-regulated.

Protein expression in response to IOERT treatment. Based on microarray data and following our assumptions regarding possible IOERT-activated cell processes, candidate proteins were selected and assayed by western blot analysis in time-course experiments after 24, 48, 72 h of exposure to 9 and 23 Gy IR doses. A peak of PLK1 expression at 24 h post-IOERT treatment and a progressive decrease at 48 and 72 h were observed in both 9 Gy- and 23 Gy-treated MCF10A cells (Figure 4). The prolonged PLK1 depletion could activate the DNA-damage checkpoint with cell-cycle arrest, as reported by Lei and Erickson (28). These observations are also in line with microarray data analysis. Moreover, at the molecular level, we did not observe an induction of intrinsic apoptotic response, as evidenced by the absence of PARP fragmentation in time-course experiments. PARP levels remained almost unchanged following both treatments (Figure 4). The extrinsic apoptotic pathway, however, seemed to be activated, as a time-dependent increase in the expression of Fas cell surface death receptor (FAS) and a simultaneous decrease in the expression of pro-caspase-8 were observed after both treatments. Finally, a compensatory activation of cellular defense mechanisms, suggested by the increased expression of p53, c-MYC, EGFR and by the mild activation of EGFR-mediated signaling pathway, as also suggested by increased phosphorylation levels of EGFR following treatments, were observed.

Discussion

Medical applications of high doses of charged particles, such as those used during IOERT, involve the exposure of normal cells, tissues and organs proximal to the tumor. The
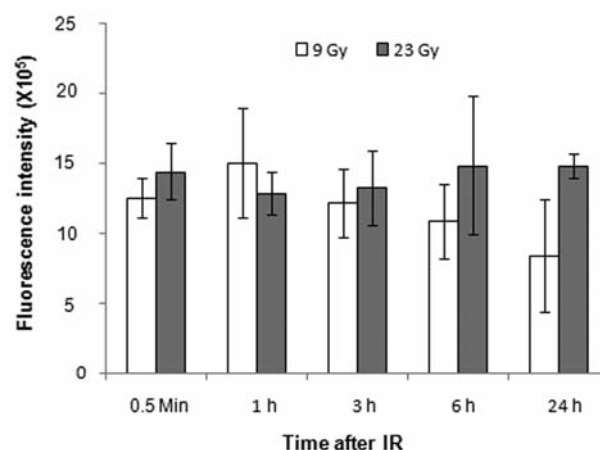

Figure 3. *Quantitative presentation of the mean gamma-H2AX fluorescence intensity for MCF10A cells 30 min, and 1, 3, 6, and 24 h after exposure to 9 and 23 Gy.*

radiobiology of healthy cells and tissue response to IR is a topic of interest which may contribute to avoiding the impairment of normal tissue and organ function and to reducing risks of secondary cancer. To date, few articles have described the biological and molecular basis of IOERT effects (22; 29-30). In particular, gene-expression profiles of breast normal cells induced by high IR doses need to be properly addressed. The purpose of the study was to analyze cell and gene expression response following IOERT treatment with 9 and 23 Gy doses (IOERT boost and exclusive, respectively) in human non-tumorigenic MCF10A mammary cell line as a model of normal breast epithelial cells. To the best of our knowledge, no studies have examined cell and gene expression changes after high-dose electron irradiation in MCF10A cells.

Firstly, we assessed cell viability in terms of reproductive capacity performing a clonogenic survival assay and observed that the 23 Gy exposure inhibited the growth and proliferation of MCF10A cells. On the contrary, following the 9-Gy boost treatment, a surviving radioresistant cell fraction with reproductive capacity was found. Immunofluorescence analyses showed that γ-H2AX foci formation rapidly increased in a dose-dependent manner following both IOERT modalities, in MCF10A cells treated with 9 Gy, the number of foci gradually decreased after-irradiation, whereas in cells treated with 23 Gy, it remained high at 24 h post-treatment. Foci formation at sites of double-strand breaks reveals the induction of DNA-repair mechanisms, however, if such damage is not adequately repaired it can lead to cell clonogenicity loss *via* the generation of lethal chromosomal aberrations, apoptotic cell death or cellular senescence (9, 12). Unlike the senescent features that we described in MCF7 cells following 9 and 23 Gy exposures (22), MCF10A cells did not show a radiation-induced senescent phenotype, as displayed
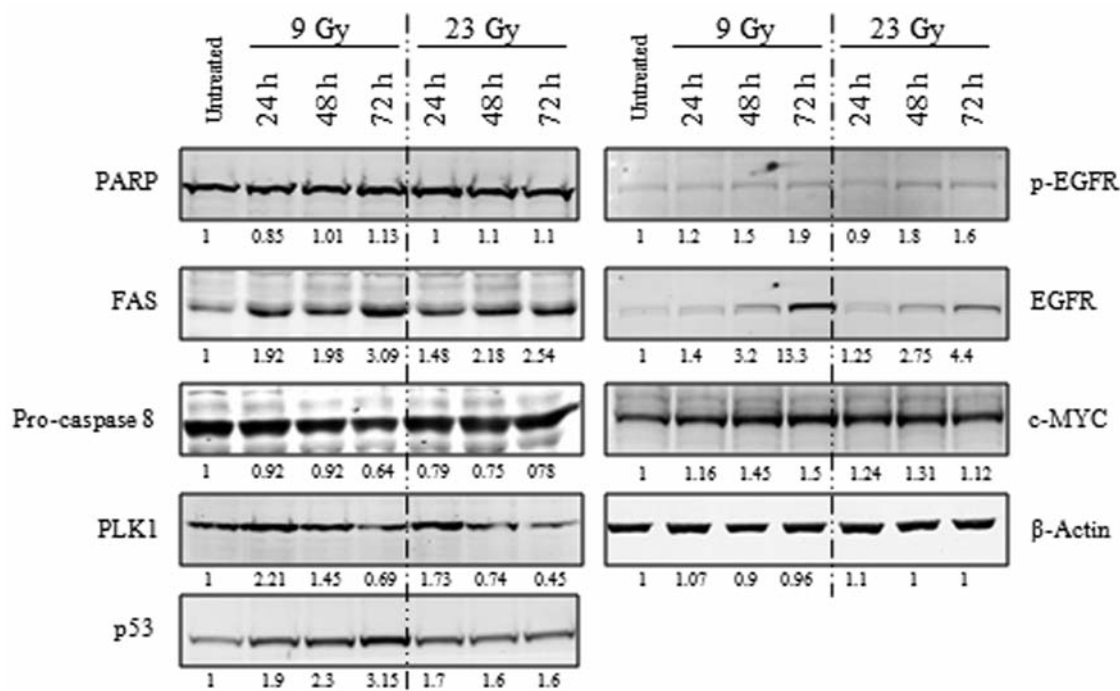
Figure 4. *Western blotting analysis for protein response factors*.

by morphological traits and by a lack of β-galactosidase activity (data not shown).

In addition, 24 h after treatments the cell networks involved in IOERT response appeared to be dose-dependent. More precisely, our results revealed that the magnitude of transcriptional variation, defined as the number of differentially expressed genes, could drive two different cell fate decisions in a dose-dependent manner. In order to highlight genes and networks activated after IOERT, we used selected validated genes to design two descriptive models for each dose delivered (Figure 5; models A and B). As reported in model A of Figure 5, the gene-expression profile of MCF10A cells treated with 9 Gy showed involvement of positive cell-cycle modulators. IR is known to activate both pro- and anti-proliferative signal pathways, producing an imbalance in the cell survival *vs*. death decision (10, 13). More precisely, MCF10A cells treated with 9 Gy activate genes involved in cell-cycle regulation, as suggested by the up-regulation of *GSTE1, PLK1, AURKA, CDC25C, CDC20, CENPF* and *KIF2C* genes. Overall, most of these genes code proteins involved in spindle formation, centrosome maturation, mitotic processes, and chromosome instability.

GTSE1 protein, localized on the microtubules, plays a role during the S/G$_2$ phase transition of the cell cycle and is significantly induced by different DNA-damaging agents, including gamma-irradiation and chemotherapeutic drugs (31). Some authors reported a down-regulation of *GTSE1* mRNA

after stress exposure such as IR, which leads to the activation of apoptotic process (31-32). Recently, GTSE1 protein was also described to play a role in promoting cell survival. In response to DNA damage, after phosphorylation mediated by PLK1, GTSE1 accumulates in the nucleus and binds the tumor-suppressor protein p53; exporting the protein from the nucleus to the cytoplasm, it represses p53 ability to induce apoptosis (33-36). In turn, our results show that *PLK1* gene was overexpressed in MCF10A cells treated with 9 Gy, this may contribute to development of the surviving radioresistant cell fraction. PLK1 represents a well-established factor that plays an important role in cell-cycle regulation, acting in centrosome maturation, spindle formation, mitotic entry and cytokinesis (37-38). On the contrary, PLK1 inhibition induces cell-cycle arrest, with subsequent cell death induction. It is interesting to note that a pre-treatment with PLK1 inhibitors sensitized human medulloblastoma cells to IR (37), thus down-regulation of the *PLK1* gene observed in MCF10A cells treated with 23 Gy could promote cell death (39-41). AURKA promotes cell-cycle progression, regulating the transition from the G$_2$ to M phase, the centrosome function and assembly of the mitotic spindle. It has also been shown to modulate the activity of tumor suppressors such as p53 and is responsible for BReast CAncer 1, early onset (BRCA1) protein phosphorylation after DNA damage (42-45). In our model, AURKA might promote cell survival following IOERT boost treatment. CDC20 and CDC25C were also up-regulated in MCF10A cells treated with
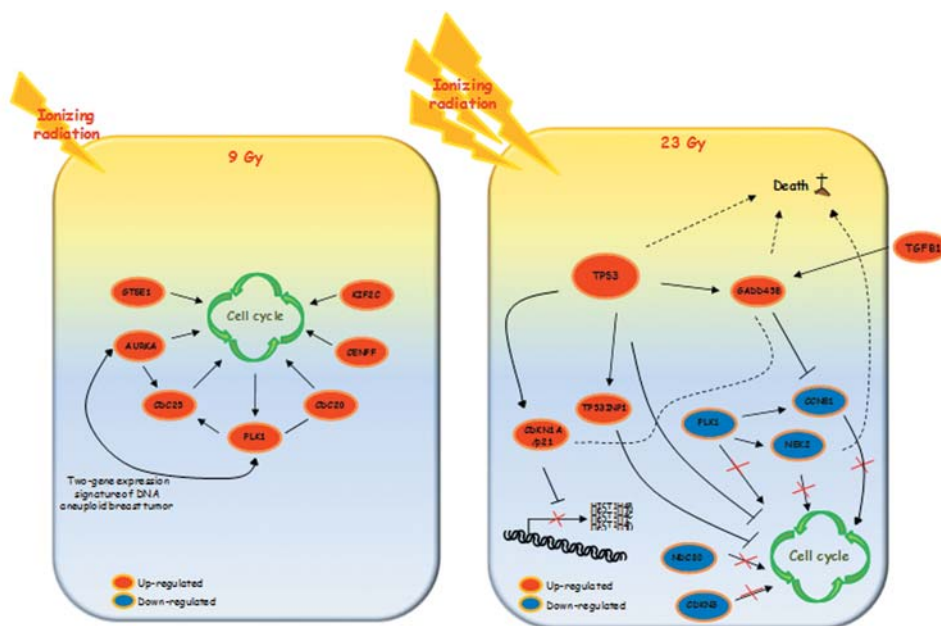
Figure 5. *Two descriptive models of genes and networks activated in MCF10A cells after Intraoperative electron radiation therapy (IOERT) using the two doses of 9 Gy (model A) and 23 Gy (model B).*

9 Gy. CDC20 appears to act as a regulatory protein, interacting with several other factors, and is required for two distinct microtubule-dependent processes: nuclear movement prior to anaphase, and chromosome separation. Moreover, CDC25C functions are to drive cell-cycle transition by de-phosphorylating and activating CDKs and to trigger entry into mitosis (22). Thus, in line with the above described gene functions, the cell cycle appears to be activated by multiple regulators after IOERT boost. CENPF and KIF2C, both up-regulated after 9-Gy exposure, have a key role during chromosome segregation in mitosis (46-48). More precisely, CENPF is involved in centromere formation and kinetochore organization during mitosis (46-51). In addition, KIF2C plays important roles in chromosome segregation and in the correction of improper kinetochore–microtubule interactions during mitosis and is regulated by aurora kinase-B (52-54).

In summary, according to our hypothesis, in MCF10A cells treated with 9 Gy, the cell cycle appears to be positively modulated at the transcriptional level by several key factors, which, to our knowledge, have never been described as being correlated to IR cell response. Furthermore, we suggest that the selected up-regulated genes, such as those involved in mitotic aberrations, should be further investigated in order to highlight their possible roles in the molecular mechanisms of mammary carcinogenesis after IR exposure (55-58).

Figure 5 also shows the descriptive model B of selected and validated genes proposed for MFC10A cells treated with 23 Gy of IR. Unlike model A, model B suggests inhibition of the cell cycle through down-regulation of its positive regulators, such as *PLK1, NDC80, CDKN3, CCNB1* and *NEK2* genes. Overall, these genes have been described as regulators of late cell-cycle phases. More precisely, the NDC80 kinetochore complex component organizes and stabilizes the microtubule-kinetochore interactions and is required for proper chromosome segregation. NDC80, together with other genes such as *CDKN3*, was found to be altered in tumor epithelial cells during malignant transformation and also correlated with poor tumor differentiation and advanced tumor stage (39, 59). CCNB1 and NEK2, both down-regulated in MCF10A cells treated with 23 Gy, have been described as regulatory factors of the cell cycle, supporting our assumption of an inhibition operating at the transcriptional level (60). In particular, it has been shown that *NEK2*-knockdown induces aneuploidy and cell-cycle arrest, ultimately leading to cell death. For these reasons, this protein was recently considered an attractive and novel therapeutic target for BC treatment (60-62).

As recently reported, IR induces down-regulation of histone mRNA levels in mammalian cells (22, 63). IR-induced inhibition of histone gene transcription depends on p21 protein expression, which was up-regulated in MCF10A cells treated with 23 Gy. It has been reported that exposure to high- and low-linear energy transfer radiation negatively regulates histone gene expression in human lymphoblastoid and colon cancer cell lines (64). In line with these data, the gene-expression profile of MCF10A cells treated with 23 Gy showed a large number of histone genes to be down-regulated. Three of these

were validated, confirming their down-regulation after a high dose of IR; to our knowledge, this result is described for the first time in breast cells (22, 63). In addition in our model B, TP53INP1, a p53-inducible gene able to modulate biological activities of p53, was up-regulated (64-69). Thus, we assayed p53 gene status by qRT-PCR and found it to be up-regulated in MCF10A cells treated with 23 Gy (6.1-fold change with respect to untreated MCF10A cells), as also shown in model B (Figure 5B) (64-69). Cell death programming seems also to be positively modulated by the up-regulation of *p53, TP53INP1, CASP8* and *GADD45B* genes (Figure 5B). Moreover, by western blot analysis, we did not observe induction of intrinsic apoptotic response, as evidenced by the absence of PARP fragmentation. PARP protein levels remained unchanged following both treatments. On the contrary, the extrinsic apoptotic pathway seemed to be activated. Indeed, a time-dependent increase in FAS expression and a simultaneous decrease of pro-caspase-8 expression was observed after both treatments in immunoblotting experiments. Moreover, GADD45B is a member of a group of genes whose transcript levels increased following stressful growth-arrest conditions and treatment with DNA-damaging agents (70). Our findings are in line with several studies that report the involvement of the above-mentioned genes in cell-fate decisions and death modulation after IR exposure (65, 71-72).

Our study, for the first time, indicates which genes are down- or up-regulated after IOERT in non-tumorigenic MCF10A cells and the molecular networks able to regulate survival or death cell decision. We highlight the involvement of well- and lesser-known genes related to the IR response, which are able to drive cell fate in opposite ways. The coded proteins might activate a complex network that positively regulates the cell cycle, promoting radioresistance in MCF10A cells treated with 9 Gy leading to a surviving cell fraction, or inhibits cell-cycle progression in MCF10A cells treated with 23 Gy. Considering their important roles in cell response to high radiation doses such as those used during IOERT, we believe that the genes identified could act as prognostic indicators for RT. For these reasons they need to be further studied in order to improve our knowledge over cell radiation effects.

Conclusion

The success of RT mainly depends on the total administered dose. This must be homogeneously delivered to the tumor and must preserve the surrounding healthy tissue. The radiobiology of the healthy tissue response to IR is a topic of interest that needs more investigation.

High-throughput methodologies, such as DNA microarray, allow the analysis of the mRNA expression of thousands of genes simultaneously in order to discover new genes and pathways as targets of response to IOERT. We observed consistent differences in transcription among the two treatments used and the magnitude of transcriptional variation was dose-dependent. We highlighted novel genes able to activate molecular networks contributing to guiding cell-fate decisions, which may provide the opportunity to explore molecular target-directed interventions in the future.

Conflicts of Interest

The Authors declare that they have no competing interests.

Acknowledgements

References

1 Orecchia R and Veronesi U: Intraoperative electrons. Semin Radiat Oncol *15*: 76-83, 2005.

2 Bernier J, Viale G, Orecchia R, Ballardini B, Richetti A, Bronz L, Franzetti-Pellanda A, Intra M and Veronesi U: Partial irradiation of the breast: Old challenges, new solutions. Breast *15(4)*: 466-475, 2006.

3 Offersen BV, Overgaard M, Kroman N and Overgaard J: Accelerated partial breast irradiation as part of breast conserving therapy of early breast carcinoma: a systematic review. Radiother Oncol *90*: 1-13, 2009.

4 Wallner P, Arthur D, Bartelink H, Connolly J, Edmundson G, Giuliano A, Goldstein N, Hevezi J, Julian T, Kuske R, Lichter A, McCormick B, Orecchia R, Pierce L, Powell S, Solin L, Vicini F, Whelan T, Wong J and Coleman CN; Workshop Participants: Workshop on partial breast irradiation: state of the art and the science. J Natl Cancer Inst *96*: 175-184, 2004.

5 Smith BD, Arthur DW, Buchholz TA, Haffty BG, Hahn CA, Hardenbergh PH, Julian TB, Marks LB, Todor DA, Vicini FA, Whelan TJ, White J, Wo JY and Harris JR: Accelerated partial breast irradiation consensus statement from the American Society for Radiation Oncology (ASTRO). Int J Radiat Oncol Biol Phys *74(4)*: 987-1001, 2009.

6 Kraus-Tiefenbacher U, Bauer L, Scheda A, Schoeber C, Schaefer J, Steil V and Wenz F: Intraoperative radiotherapy (IORT) is an option for patients with localized breast recurrences after previous external-beam radiotherapy. BMC Cancer *14;7*: 178, 2007.

7 Veronesi U, Orecchia R, Luini A, Galimberti V, Zurrida S, Intra M, Veronesi P, Arnone P, Leonardi MC, Ciocca M, Lazzari R, Caldarella P, Rotmensz N, Sangalli C, Sances D and Maisonneuve P: Intraoperative radiotherapy during breast conserving surgery: a study on 1,822 cases treated with electrons. Breast Cancer Res Treat *124(1)*: 141-151, 2010.

8 Zhao W, Diz DI and Robbins ME: Oxidative damage pathways in relation to normal tissue injury. Br J Radiol 80 Spec No *1*: S23-31, 2007.

9 Lomax ME, Folkes LK and O'Neill P: Biological consequences of radiation-induced DNA damage: relevance to radiotherapy. Clin Oncol (R Coll Radiol) *25*: 578-785, 2013.

10 Multhoff G and Radons J: Radiation, inflammation, and immune responses in cancer. Front Oncol *2*: 58, 2012.

11 Eriksson D and Stigbrand T: Radiation-induced cell death mechanisms. Tumor Biol *31*: 363-372, 2010.

12 Surova O and Zhivotovsky B: Various modes of cell death induced by DNA damage. Oncogene *32*: 3789-3797, 2013.

13 Golden EB, Pellicciotta I, Demaria S, Barcellos-Hoff MH and Formenti SC: The convergence of radiation and immunogenic cell death signaling pathways. Front Oncol *2*: 88, 2012.

14 West CM and Barnett GC: Genetics and genomics of radiotherapy toxicity: towards prediction. Genome Med 3(8): 52, 2011.

15 Xu QY, Gao Y, Liu Y, Yang WZ and Xu XY: Identification of differential gene expression profiles of radioresistant lung cancer cell line established by fractionated ionizing radiation *in vitro*. Chin Med J (Engl) *121*: 1830-1837, 2008.

16 Snyder AR and Morgan WF: Gene expression profiling after irradiation: clues to understanding acute and persistent responses? Cancer Metastasis Rev *23*: 259-268, 2004.

17 Minafra L and Bravatà V: Cell and molecular response to IORT treatment. Transl Cancer Res *3(1)*: 32-47, 2014. doi: 10.3978/j.issn.2218-676X.2014.02.03.

18 Bravatà V, Cammarata FP, Forte GI and Minafra L: "Omics" of HER2-positive breast cancer. OMICS *17*: 119-129, 2013.

19 Bravatà V, Stefano A, Cammarata FP, Minafra L, Russo G, Nicolosi S, Pulizzi S, Gelfi C, Gilardi MC and Messa C: Genotyping analysis and 18F-FDG uptake in breast cancer patients: a preliminary research. J Exp Clin Cancer Res *32*: 23, 2013.

20 Minafra L, Norata R, Bravatà V, Viola M, Lupo C, Gelfi C and Messa C: Unmasking epithelial–mesenchymal transition in a breast cancer primary culture: a study report. BMC Res Notes *5*: 343, 2012.

21 Minafra L, Bravatà V, Forte GI, Cammarata FP, Gilardi MC and Messa C: Gene expression profiling of epithelial–mesenchymal transition in primary breast cancer cell culture. Anticancer Res *34(5)*: 2173-2183, 2014.

22 Bravatà V, Minafra L, Russo G, Forte GI, Cammarata FP, Ripamonti M, Casarino C, Augello G, Costantini F, Barbieri G, Messa C and Gilardi MC: High-dose ionizing radiation regulates gene expression changes in MCF7 breast cancer cell line. Anticancer Res *35*: 5, 2015. In press.

23 Franken NAP, Rodermond HM, Stap J, Haveman J and van Bree C: Clonogenic assay of cells *in vitro*. Nature Protocols *1*: 2315-2319, 2006.

24 Edgar R, Domrachev M and Lash AE: Gene Expression Omnibus: NCBI gene expression and hybridization array data repository. Nucleic Acids Res *30(1)*: 207-210, 2002.

25 Rozen S and Skaletsky HJ: Primer3 on the WWW for general users and for biologist programmers. *In*: Bioinformatics Methods and Protocols: Methods in Molecular Biology. Krawetz S and Misener S (eds.). Humana Press, Totowa, NJ, pp. 365-386, 2000.

26 Primer3 tool. http//fokker.wi.mit.edu/primer3.

27 Becker KG, Hosack DA, Dennis G Jr., Lempicki RA, Bright TJ, Cheadle C and Engel J: PubMatrix: a tool for multiplex literature mining. BMC Bioinformatics *10*: 4: 61, 2003.

28 Lei M and Erikson RL: Plk1 depletion in non transformed diploid cells activates the DNA-damage checkpoint. Oncogene *27*: 3935-3943, 2008.

29 Di Maggio FM, Minafra L, Forte GI, Cammarata FP, Lio D, Messa C, Gilardi MC and Bravatà V: Portrait of inflammatory response to ionizing radiation treatment. J Inflamm *12*: 14, 2015.

30 Herskind C and Wenz F: Radiobiological aspects of intraoperative tumour-bed irradiation with low-energy X-rays (LEX-IORT). Transl Cancer Res *3*: 3-17, 2014.

31 Monte M, Collavin L, Lazarevic D, Utrera R, Dragani TA and Schneider C: Cloning, chromosome mapping and functional characterization of a human homologue of murine Gtse-1 (B99) gene. Gene *254(1-2)*: 229-236, 2000.

32 Yong KJ, Milenic DE, Baidoo KE, Kim YS and Brechbiel MW: Gene expression profiling upon (212) Pb-TCMC-trastuzumab treatment in the LS-174T i.p. xenograft model. Cancer Med *2(5)*: 646-653, 2013.

33 Tian T, Zhang E, Fei F, Li X, Guo X, Liu B, Li J, Chen Z and Xing J: Up-regulation of GTSE1 lacks a relationship with clinical data in lung cancer. Asian Pac J Cancer Prev *12(8)*: 2039-2043, 2011.

34 Collavin L, Monte M, Verardo R, Pfleger C and Schneider C: Cell-cycle regulation of the p53-inducible gene B99. FEBS Lett *481(1)*: 57-62, 2000.

35 Monte M, Benetti R, Buscemi G, Sandy P, Del Sal G and Schneider C: The cell cycle-regulated protein human GTSE-1 controls DNA damage-induced apoptosis by affecting p53 function. J Biol Chem *278(32)*: 30356-30364, 2003.

36 Liu XS, Li H, Song B and Liu X: Polo-like kinase 1 phosphorylation of G2 and S-phase-expressed 1 protein is essential for p53 inactivation during G2 checkpoint recovery. EMBO Rep *11(8)*: 626-632, 2010.

37 Harris PS, Venkataraman S, Alimova I, Birks DK, Donson AM, Knipstein J, Dubuc A, Taylor MD, Handler MH, Foreman NK and Vibhakar R: Polo-like kinase 1 (PLK1) inhibition suppresses cell growth and enhances radiation sensitivity in medulloblastoma cells. BMC Cancer *12*: 80, 2012.

38 Strebhardt K: Multifaceted polo-like kinases: drug targets and antitargets for cancer therapy. Nat Rev Drug Discov *9(8)*: 643-660, 2010.

39 Bièche I, Vacher S, Lallemand F, Tozlu-Kara S, Bennani H, Beuzelin M, Driouch K, Rouleau E, Lerebours F, Ripoche H, Cizeron-Clairac G, Spyratos F and Lidereau R: Expression analysis of mitotic spindle checkpoint genes in breast carcinoma: role of NDC80/HEC1 in early breast tumorigenicity, and a two-gene signature for aneuploidy. Mol Cancer *10*: 23, 2011.

40 Korkola JE, Blaveri E, DeVries S, Moore DH, Hwang ES, Chen YY, Estep AL, Chew KL, Jensen RH and Waldman FM: Identification of a robust gene signature that predicts breast cancer outcome in independent data sets. BMC Cancer *7*: 61, 2007.

41 Morris SR and Carey LA: Gene-expression profiling in breast cancer. Curr Opin Oncol *19*: 547-551, 2007.

42 Siggelkow W, Boehm D, Gebhard S, Battista M, Sicking I, Lebrecht A, Solbach C, Hellwig B, Rahnenführer J, Koelbl H, Gehrmann M, Marchan R, Cadenas C, Hengstler JG and Schmidt M: Expression of aurora kinase A is associated with metastasis-free survival in node-negative breast cancer patients. BMC Cancer *12*: 562, 2012.

43 Keen N and Taylor S: Aurora-kinase inhibitors as anticancer agents. Nat Rev Canc 4: 927-936, 2004.

44 Marumoto T, Zhang D and Saya H: Aurora-A – a guardian of poles. Nat Rev Canc 5: 42-50, 2005.

45 Ouchi M, Fujiuchi N, Sasai K, Katayama H, Minamishima YA, Ongusaha PP, Deng C, Sen S, Lee SW and Ouchi T: BRCA1 phosphorylation by aurora-A in the regulation of G2 to M transition. J Biol Chem *279*: 19643-19648, 2004.

46 Cao JY, Liu L, Chen SP, Zhang X, Mi YJ, Liu ZG, Li MZ, Zhang H, Qian CN, Shao JY, Fu LW, Xia YF and Zeng MS: Prognostic significance and therapeutic implications of centromere protein F expression in human nasopharyngeal carcinoma. Mol Cancer 9: 237, 2010.

47 Brendle A, Brandt A, Johansson R, Enquist K, Hallmans G, Hemminki K, Lenner P and Försti A: Single nucleotide polymorphisms in chromosomal instability genes and risk and clinical outcome of breast cancer: a Swedish prospective case–control study. Eur J Cancer 45(3): 435-442, 2009.

48 Campone M, Campion L, Roché H, Gouraud W, Charbonnel C, Magrangeas F, Minvielle S, Genève J, Martin AL, Bataille R and Jézéquel P: Prediction of metastatic relapse in node-positive breast cancer: establishment of a clinicogenomic model after FEC100 adjuvant regimen. Breast Cancer Res Treat 109(3): 491-501, 2008.

49 Bomont P, Maddox P, Shah JV, Desai AB and Cleveland DW: Unstable microtubule capture at kinetochores depleted of the centromere-associated protein CENP-F. EMBO J 24: 3927-3939, 2005.

50 Holt SV, Vergnolle MA, Hussein D, Wozniak MJ, Allan VJ and Taylor SS: Silencing Cenp-F weakens centromeric cohesion, prevents chromosome alignment and activates the spindle checkpoint. J Cell Sci 118: 4889-4900, 2005.

51 O'Brien SL, Fagan A, Fox EJ, Millikan RC, Culhane AC, Brennan DJ, McCann AH, Hegarty S, Moyna S, Duffy MJ, Higgins DG, Jirström K, Landberg G and Gallagher WM: CENP-F expression is associated with poor prognosis and chromosomal instability in patients with primary breast cancer. Int J Cancer 120: 1434-1443, 2007.

52 Shimo A, Tanikawa C, Nishidate T, Lin ML, Matsuda K, Park JH, Ueki T, Ohta T, Hirata K, Fukuda M, Nakamura Y and Katagiri T: Involvement of kinesin family member 2C/mitotic centromere-associated kinesin overexpression in mammary carcinogenesis. Cancer Sci 99(1): 62-70, 2008.

53 Andrews PD, Ovechkina Y, Morrice N, Wagenbach M, Duncan K, Wordeman L and Swedlow JR: Aurora B regulates MCAK at the mitotic centromere. Dev Cell 6: 253-268, 2004.

54 Lan W, Zhang X, Kline-Smith SL, Rosasco SE, Barrett-Wilt GA, Shabanowitz J, Hunt DF, Walczak CE and Stukenberg PT: Aurora B phosphorylates centromeric MCAK and regulates its localization and microtubule depolymerization activity. Curr Biol 14: 273-286, 2004.

55 Olson JE, Wang X, Pankratz VS, Fredericksen ZS, Vachon CM, Vierkant RA, Cerhan JR and Couch FJ: Centrosome-related genes, genetic variation, and risk of breast cancer. Breast Cancer Res Treat 125(1): 221-228, 2011.

56 D'Assoro AB, Lingle WL and Salisbury JL: Centrosome amplification and the development of cancer. Oncogene 21(40): 6146-6153, 2002.

57 Brinkley BR: Managing the centrosome numbers game: from chaos to stability in cancer cell division. Trends Cell Biol 11(1): 18-21, 2001.

58 Marx J: Cell biology: Do centrosome abnormalities lead to cancer? Science 292(5516): 426-429, 2001.

59 Xing C, Xie H, Zhou L, Zhou W, Zhang W, Ding S, Wei B, Yu X, Su R and Zheng S: Cyclin-dependent kinase inhibitor 3 is overexpressed in hepatocellular carcinoma and promotes tumor cell proliferation. Biochem Biophys Res Commun 420(1): 29-35, 2012.

60 Lee J and Gollahon L: NEK2-Targeted ASO or siRNA pretreatment enhances anticancer drug sensitivity in triple-negative breast cancer cells. Int J Oncol 42(3): 839-847, 2013.

61 Cappello P, Blaser H, Gorrini C, Lin DC, Elia AJ, Wakeham A, Haider S, Boutros PC, Mason JM, Miller NA, Youngson B, Done SJ and Mak TW: Role of NEK2 on centrosome duplication and aneuploidy in breast cancer cells. Oncogene 33(18): 2375-2384, 2014.

62 Wu G, Qiu XL, Zhou L, Zhu J, Chamberlin R, Lau J, Chen PL and Lee WH: Small molecule targeting the Hec1/Nek2 mitotic pathway suppresses tumor cell growth in culture and in animal. Cancer Res 68(20): 8393-8399, 2008.

63 Su C, Gao G, Schneider S, Helt C, Weiss C, O'Reilly MA, Bohmann D and Zhao J: DNA damage induces down regulation of histone gene expression through the G1 checkpoint pathway. EMBO J 23(5): 1133-1143, 2004.

64 Meador JA, Ghandhi SA and Amundson SA: p53-independent down-regulation of histone gene expression in human cell lines by high- and low-let radiation. Radiat Res 175(6): 689-699, 2011.

65 Jiang PH, Motoo Y, Garcia S, Iovanna JL, Pébusque MJ and Sawabu N: Down-regulated expression of tumor protein p53-induced nuclear protein 1 in human gastric cancer. World J Gastroenterol 12(5): 691-696, 2006.

66 Tomasini R, Samir AA, Vaccaro MI, Pebusque MJ, Dagorn JC, Iovanna JL and Dusetti NJ: Molecular and functional characterization of the stress-induced protein (SIP) gene and its two transcripts generated by alternative splicing. SIP induced by stress and promotes cell death. J Biol Chem 276: 44185-44192, 2001.

67 Tomasini R, Samir AA, Pebusque MJ, Calvo EL, Totaro S, Dagorn JC, Dusetti NJ and Iovanna JL: P53-dependent expression of the stress-induced protein (SIP). Eur J Cell Biol 81: 294-301, 2002.

68 Tomasini R, Samir AA, Carrier A, Isnardon D, Cecchinelli B, Soddu S, Malissen B, Dagorn JC, Iovanna JL and Dusetti NJ: TP53INP1s and homeodomain-interacting protein kinase-2 (HIPK2) are partners in regulating p53 activity. J Biol Chem 278: 37722-37729, 2003.

69 Okamura S, Arakawa H, Tanaka T, Nakanishi H, Ng CC, Taya Y, Monden M and Nakamura Y: p53DINP1, a p53-inducible gene, regulates p53-dependent apoptosis. Mol Cell 8: 85-94, 2001.

70 Heminger K, Jain V, Kadakia M, Dwarakanath B and Berberich SJ: Altered gene expression induced by ionizing radiation and glycolytic inhibitor 2-deoxy-glucose in a human glioma cell line: implications for radio sensitization. Cancer Biol Ther 5(7): 815-23, 2006.

71 Chen T, Chen M and Chen J: Ionizing radiation potentiates dihydroartemisinin-induced apoptosis of A549 cells via a caspase-8-dependent pathway. PLoS One 8(3): e59827, 2013.

72 Luce A, Courtin A, Levalois C, Altmeyer-Morel S, Romeo PH, Chevillard S and Lebeau J: Death receptor pathways mediate targeted and non-targeted effects of ionizing radiations in breast cancer cells. Carcinogenesis 30(3): 432-439, 2009.